Journal of Luminescence 128 (2008) 1927–1936

Contents lists available at ScienceDirect

Journal of Luminescence

journal homepage: www.elsevier.com/locate/jlumin

Structure and linear spectroscopic properties of near IR polymethine dyes

Scott Webster [a,*], Lazaro A. Padilha [a], Honghua Hu [a], Olga V. Przhonska [a,c], David J. Hagan [a,b], Eric W. Van Stryland [a,b], Mikhail V. Bondar [c], Iryna G. Davydenko [d], Yuriy L. Slominsky [d], Alexei D. Kachkovski [d]

[a] CREOL & FPCE, The College of Optics and Photonics, University of Central Florida, Orlando, FL 32816, USA
[b] Department of Physics, University of Central Florida, Orlando, FL 32816, USA
[c] Institute of Physics, National Academy of Sciences, Prospect Nauki 46, Kiev 03028, Ukraine
[d] Institute of Organic Chemistry, National Academy of Sciences, Murmanskaya 5, Kiev 03094, Ukraine

ARTICLE INFO

Article history:
Received 13 February 2008
Received in revised form
29 April 2008
Accepted 3 June 2008
Available online 6 June 2008

Keywords:
Polymethine
Structure–property relations
Solvatochromism
Quantumchemical analysis
Symmetry breaking
Absorption
Fluorescence
Cyanine
Terminal groups
Squaraine
Tetraone
Organic dyes
Visible
Near infrared
Red shift
Solvent-dependent
Chromophore
Charge delocalization
Weak fluorescence
Excited states

ABSTRACT

We performed a detailed experimental investigation and quantum-chemical analysis of a new series of near IR polymethine dyes with 5-butyl-7,8-dihydrobenzo[*cd*]furo[2,3-*f*]indolium terminal groups. We also synthesized and studied two neutral dyes, squaraine and tetraone, with the same terminal groups and performed a comparison of the spectroscopic properties of this set of "near IR" dyes (polymethine, squaraine, and tetraone) with an analogous set of "visible" dyes with simpler benzo[*e*]indolium terminal groups. From these measurements, we find that the dyes with dihydrobenzo[*cd*]furo[2,3-*f*]indolium terminal groups are characterized by a remarkably large shift $\approx$300 nm ($\approx$200 nm for tetraone) of their absorption bands towards the red region. We discuss the difference in electronic structure for these molecules and show that the "near IR" dyes are characterized by an additional weak fluorescence band from the higher lying excited states connected with the terminal groups. Absorption spectra for the longest polymethines are solvent-dependent and are characterized by a broadening of the main band in polar solvents, which is explained by ground state symmetry breaking and reduced charge delocalization within the polymethine chromophore. The results of these experiments combined with the agreement of quantum chemical calculations moves us closer to a predictive capability for structure–property relations in cyanine-like molecules.

1. Introduction

Cyanine and cyanine-like dyes have been known for more than a century and have found numerous applications as photosensitizers in photography and photodynamic therapy, fluorescent probes in chemistry and biology, active and passive laser media, materials for electroluminescence and nonlinear optics, etc. [1,2]. They are among a particular class of organic compounds that exhibit a strong and tunable absorption in the near infrared (NIR) region, which is important for the development of organic materials with large third-order nonlinearities for all-optical signal processing [3]. This long wavelength absorption can be obtained using two methods: lengthening the polymethine chromophore (polymethine chain) or introducing specific terminal groups with their own extended conjugation system, which can strongly interact with the main chromophore and extend the total effective length of conjugation in the molecule [4]. The first method typically decreases photostability of the molecules, which can be partially improved by the introduction of bridge units within the chain [5]. However, the second method allows significant shifting of the absorption bands towards the red region without a substantial decrease of the photochemical stability. In

* Corresponding author.
E-mail address: swebster@creol.ucf.edu (S. Webster).

0022-2313/$ - see front matter © 2008 Elsevier B.V. All rights reserved.
doi:10.1016/j.jlumin.2008.06.002

addition to the significant practical importance, our interest in studying these near IR dyes is driven by multiple theoretical questions:

1. How to understand the origin of charge localization on some specific molecular orbitals, so called local orbitals, which are connected with the terminal group structures and their interaction with the conjugation chain?
2. How to understand the role of these local molecular orbitals in linear and nonlinear absorption?
3. What is the origin of the extensive broadening of the absorption spectra for near IR dyes in polar solvents, which is connected with a symmetry breaking effect and reduced charge delocalization within the polymethine chromophore [6–12]?

In order to find answers to these questions, we synthesized [13,14] and studied a series of cationic cyanines with 5-butyl-7,8-dihydrobenzo[*cd*]furo[2,3-*f*]indolium terminal groups, which are characterized by their own extended π-conjugated system strongly connected to the conjugated system of the chain. We show that these dyes are characterized by linear absorption bands shifted to the long wavelength region by up to ~300 nm as compared to the dyes with the same length of the chain but simpler terminal groups such as indolium or benzo[*e*]indolium, studied by us earlier [15,16]. We synthesized and studied two additional neutral dyes, squaraine and tetraone, with analogous structures to provide a deeper insight into structure–property relations and get a better understanding of the properties of cyanine and cyanine-like molecules.

In the current paper we describe: (1) the electronic structure of the near IR dyes, (2) absorption and fluorescence properties in solvents of different polarity, (3) a detailed comparison with our previously studied dyes in the visible region, and (4) quantum-chemical analysis allowing us to understand the nature of their linear absorption bands. The combination of spectroscopic methods with quantum-chemical calculations gives us information about the level structure and furthers our understanding of the optical properties in cyanine-like molecules, which are important for nonlinear optical applications [15,16].

2. Results and discussion

2.1. Materials characterization and spectroscopic properties

The molecular structures of the dyes studied in this paper are shown in Figs. 1–3. Their chemical names are: 5-butyl-4-[3-(5-butyl-8-methyl-7,8-dihydrobenzo[*cd*]furo[2,3-*f*]indol-4(5*H*)-ylidene)-prop-1-enyl]-8-methyl-7,8-dihydrobenzo[*cd*]furo[2,3-*f*]indol-5-ium tetrafluoro-borate (labeled as PD 2371); 5-butyl-4-[5-(5-butyl-8-methyl-7,8-dihydrobenzo[*cd*]furo[2,3-*f*]indol-4(5*H*)-ylidene) penta-1,3-dienyl]-8-methyl-7,8-dihydrobenzo[*cd*]furo[2,3-*f*]indol-5-iumtetrafluoroborate (labeled as PD 2658), 5-butyl-4-[7-(5-butyl-8-methyl-7,8-dihydrobenzo-[*cd*]furo[2,3-*f*]indol-4(5*H*)-ylidene) hepta-1,3,5-trienyl]-8-methyl-7,8-dihydrobenzo[*cd*]furo[2,3-*f*] indol-5-ium tetrafluoroborate (labeled as PD 2716), 5-butyl-4-(3-{3-[3-(5-butyl-8-methyl-7,8-dihydrobenzo[*cd*]furo[2,3-*f*]indol-4(5*H*)-ylidene)prop-1-enyl]-5,5-dimethylcyclohex-2-en-1-ylidene}prop-1-enyl)-8-methyl-7,8-dihydrobenzo[*cd*]furo[2,3-*f*]indol-5-ium tetrafluoroborate (labeled as PD 2892). These dyes differ by the length of polymethine chromophore (number of vinylene groups $n = 1$, 2, 3 and 4). The corresponding tetracarbocyanine PD 2892 includes a trimethylene bridge in the chromophore to increase thermal and photostability. A salt, labeled as 2337, with an analogous structure to the dihydrobenzo[*cd*]furo[2,3-*f*]indolium terminal groups was studied and compared to the corresponding dyes. Based on the structure of dicarbocyanine PD 2658, two new compounds, squaraine 4-[(5-butyl-8-methyl-7,8-dihydrobenzo[*cd*] furo[2,3-*f*]indol-5-ium-4-yl)methylene]-2-[(5-butyl-8-methyl-7, 8-dihydrobenzo[*cd*]furo[2,3-*f*]indol-4(5*H*)-ylidene)methyl]-3-oxo-cyclobut-1-en-1-olate (labeled as SD 2878) and tetraone 3,6-bis [2-(5-butyl-8-methyl-7,8-dihydrobenzo[*cd*]furo[2,3-*f*]indol-4(5*H*)-ylidene)ethylidene]cyclohexane-1,2,4,5-tetrone (labeled as TD 2824), were synthesized and investigated. The two last molecules possess identical terminal groups and similar lengths of conjugation for the purpose of performing a comparative analysis of the influence of increasing the acceptor bridge strength on the optical properties. We also perform a comparison of the spectroscopic properties of this new set of "near IR" dyes (PD 2658, SD 2878, and TD 2824) with a set of "visible" dyes (PD 2630, SD 2243, and TD 2765) which were investigated by us earlier [15–17]. The extinction coefficients for the dyes investigated in butanol are: $0.99 \times 10^5\,M^{-1}\,cm^{-1}$ at a peak position of 885 nm for PD 2371, $2.11 \times 10^5\,M^{-1}\,cm^{-1}$ at a peak position of 980 nm for PD 2658, $1.37 \times 10^5\,M^{-1}\,cm^{-1}$ at a peak position of 1096 nm for PD 2716, $1.18 \times 10^5\,M^{-1}\,cm^{-1}$ at a peak position of 1223 nm for PD 2892, $1.71 \times 10^5\,M^{-1}\,cm^{-1}$ at a peak position of 963 nm for SD 2878, and $1.76 \times 10^5\,M^{-1}\,cm^{-1}$ at a peak position of 813 nm for TD 2824.

The linear absorption and fluorescence spectra of all molecules are studied in spectroscopic grade solvents of different polarity (purchased from Sigma–Aldrich): acetonitrile CH_3CN, dimethyl sulfoxide C_2H_6OS, butanol C_4H_9OH, dichloromethane CH_2Cl_2 and *o*-dichlorobenzene $C_6H_4Cl_2$. All spectra are recorded with a Varian Cary 500 spectrophotometer and PTI QuantaMaster spectrofluorimeter equipped with a nitrogen cooled (77 K) Hamamatsu R5509-73 photomultiplier as shown in Figs. 1–3. All fluorescence spectra are corrected with the spectral responsivity of the photomultiplier. It is known that the polarity of solvents can be characterized by their orientational polarizability, which is given by $\Delta f = (\varepsilon-1)/(2\varepsilon+1)-(n^2-1)/(2n^2+1)$, where ε is the static dielectric constant and n is the refractive index of the solvent [18]. Calculated Δf values range from the smallest polarity 0.208 for $C_6H_4Cl_2$ (cationic dyes cannot be dissolved in solvents of lower polarity) to the largest in this series 0.305 for CH_3CN. It is known that relatively short wavelength absorbing PDs exhibit classic nonpolar solvatochromism: a red shift in absorption peak with an increase in solvent polarity, which correlates with a decrease in their refractive index. This is consistent with a symmetrical ground and excited state charge distribution and small permanent dipole moments ($\mu_0 = 1$–2 D) oriented perpendicular to the polymethine chromophore [8,18]. In contrast, absorption spectra of PDs absorbing in the range of ≈1000 nm demonstrate a strong dependence on solvent polarity. As was shown by us previously [7], an increase in solvent polarity leads to substantial band broadening represented by the growth of the short wavelength shoulder. This is a strong indication of polar solvatochromism, which is typical for dyes that exhibit charge localization and a large ground-state permanent dipole moment [8]. This effect was investigated by us theoretically [9] and experimentally for the symmetrical pentacarbocyanine PD 1659 and explained by a symmetry breaking effect leading to the appearance of a ground-state structural form with asymmetrical charge distribution and thus an asymmetrical bond length alternation [7]. Our explanation is based on the previously proposed theoretical concept of the formation of charge density waves (or solitonic waves) in the linear conjugated polymethine chromophores [11,12]. We assume that if the width of the solitonic wave (15–17 carbon atoms) exceeds the dimensions of the dye molecule, then only the symmetric charge distribution can be detected. In this case, PDs show the typical spectral behavior such as a narrow and intense

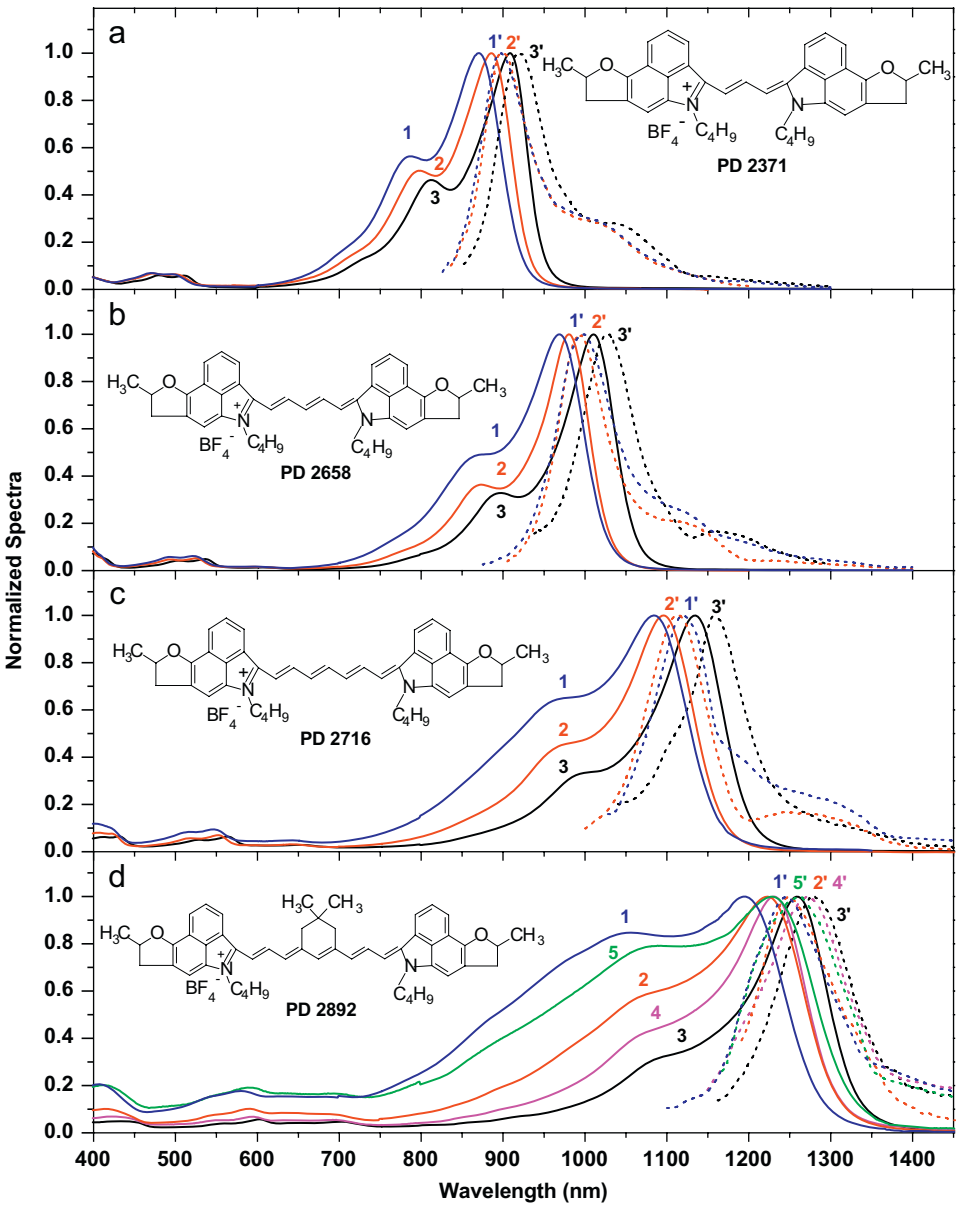

Fig. 1. Molecular structures, absorption (solid lines 1, 2, 3, 4, 5) and fluorescence spectra (dashed lines 1′, 2′, 3′, 4′, 5′) for PD 2371 (a), PD 2658 (b), PD 2716 (c), and PD 2892 (d) in acetonitrile (1, 1′), butanol (2, 2′), dichlorobenzene (3, 3′), methylene chloride (4, 4′) and dimethyl sulfoxide (5, 5′) respectively.

absorption band, nonpolar solvatochromism, a regular red shift of the band with lengthening of the chain without a substantial change of its half width. If the width of the solitonic wave becomes comparable to the length of the polymethine chain, then both the symmetrical and asymmetrical charge distributions can be detected as a function of the solvent properties. This leads to dramatic changes in the spectral characteristics of the near IR dyes. The main spectral characteristics of PDs 2371, 2658, 2716, 2892, SD 2878, and TD 2824 in different solvents are summarized in Table 1.

Our quantum-chemical calculations (HyperChem package, AM1 method) show that the symmetry of molecular geometry is conserved for near IR PDs with dihydrobenzo[*cd*]furo[2,3-*f*]indolium terminal groups for $n = 1$, 2, and 3. For example, for tricarbocyanine PD 2716, the bond lengths within the chain equidistant from the center of the chromophore are calculated to be: 1.393, 1.393, 1.399, 1.393, 1.393, 1.399, 1.393, and 1.393 Å. Note that the bond lengths are symmetric about the center of the chain. However, for longer molecules, starting from $n = 4$, calculations show an inequality of the corresponding bond lengths. Thus, for tetracarbocyanine PD 2892 they are the following: 1.404, 1.383, 1.399, 1.390, 1.419, 1.381, 1.426, 1.368, 1.413, and 1.377 Å, indicating a symmetry breaking effect. Note that here the bond lengths are asymmetric. We note that substantial broadening of the absorption band in polar CH_3CN is observed even for tricarbocyanine PD 2716 ($n = 3$), shown in Fig. 1 where all the other dyes are also shown. Therefore, we suggest that experimentally, the existence of the asymmetrical form may be observed in this series of polymethines starting from $n = 3$. An increase in solvent polarity shifts the equilibrium between these two forms to favor the asymmetrical form. Experiments show that the less polar solvent, $C_6H_4Cl_2$, primarily stabilizes the symmetric form.

2.2. Fluorescence and quantum yield measurements

In contrast to the absorption spectra, fluorescence spectra for all PDs are similarly narrow, independent of the solvent polarity,

indicating that emission originates from the symmetrical form only. The largest Stokes shift (300–350 cm^{-1}) corresponds to the most polar solvent, CH_3CN. Interestingly, these dyes also show fluorescence from higher lying excited states, this "blue" fluorescence is much less intense than the main fluorescence band and is placed in the range of 500–650 nm. This is unusual since most fluorophores fluoresce from the bottom of the first excited state, a common principle known as Kasha's rule. Great care in purification has been taken to insure the validity of this "blue" fluorescence by removing any synthesis impurities. Our explanation is that the "blue" fluorescence originates from the local orbitals connected with the terminal groups since the emission spectrum is quite similar to the emission of the salt 2337, as presented in Fig. 2. Quantum-chemical analysis, described in Section 3, gives an additional confirmation of the nature of this "blue" fluorescence. Fluorescence excitation anisotropy was performed by the standard method [18,19] and is nearly constant over the main absorption band. Even in low viscosity solvents, we measure high anisotropy values of ≈0.4. This suggests that the fluorescence lifetimes are short compared to the reorientation lifetimes, which are typically 300–500 ps [20].

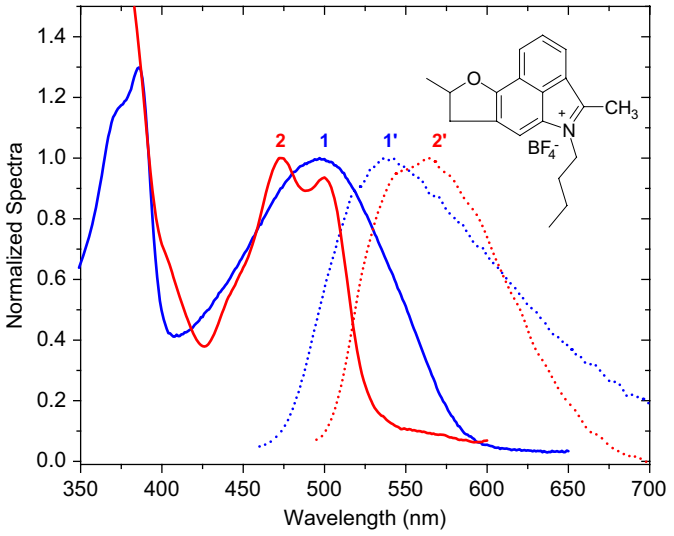

Fig. 2. Molecular structure, absorption (solid lines 1, 2) and fluorescence spectra (dashed lines 1′, 2′) of the salt 2337 (1, 1′) in comparison with the UV absorption (2) and "blue" fluorescence (2′) of PD 2371 in butanol solutions.

The absorption and fluorescence spectra of SD 2878 ($n = 2$) and TD 2824 ($n = 2$) in butanol are shown in Fig. 3. PD 2658 and SD 2878 have the same donor (D) terminal groups, the same chain length with an odd number of carbon atoms, however, the squaraine molecule includes an acceptor (A) bridge in the main conjugation backbone and therefore represents the structure: D–π–A–π–D. The tetraone dye TD 2824 belongs to a polyene-like family of compounds with an even number of carbon atoms in the conjugated chain. Having the same terminal groups and similar length of the chromophore, this dye contains a stronger acceptor bridge. The absorption bands of SD 2878 and TD 2824 (especially TD 2824 as a polyene structure) are blue shifted when compared to the corresponding PD 2658. These shifts correlate with increasing electron acceptor strength in the bridge leading to a decrease in effective conjugation length due to bond lengthening in the acceptor groups. Fluorescence spectra have approximately mirror symmetry, indicating similar vibrational structures of the ground and first excited state singlets, with a Stokes shift of ~150–250 cm^{-1}.

Fluorescence quantum yields are measured using the standard method of comparison with a known fluorophore's quantum yield. Note that there are currently no fluorescence quantum yield standards for the near IR region. The most "red" known standard is Cresyl Violet Perchlorate (Sigma–Aldrich, CAS #41830-80-2) in methanol with an absorption peak at 594 nm, a fluorescence peak at 620 nm, and a quantum yield of $\eta = 0.54$ [21]. Therefore, quantum yield measurements for the molecules in the near IR

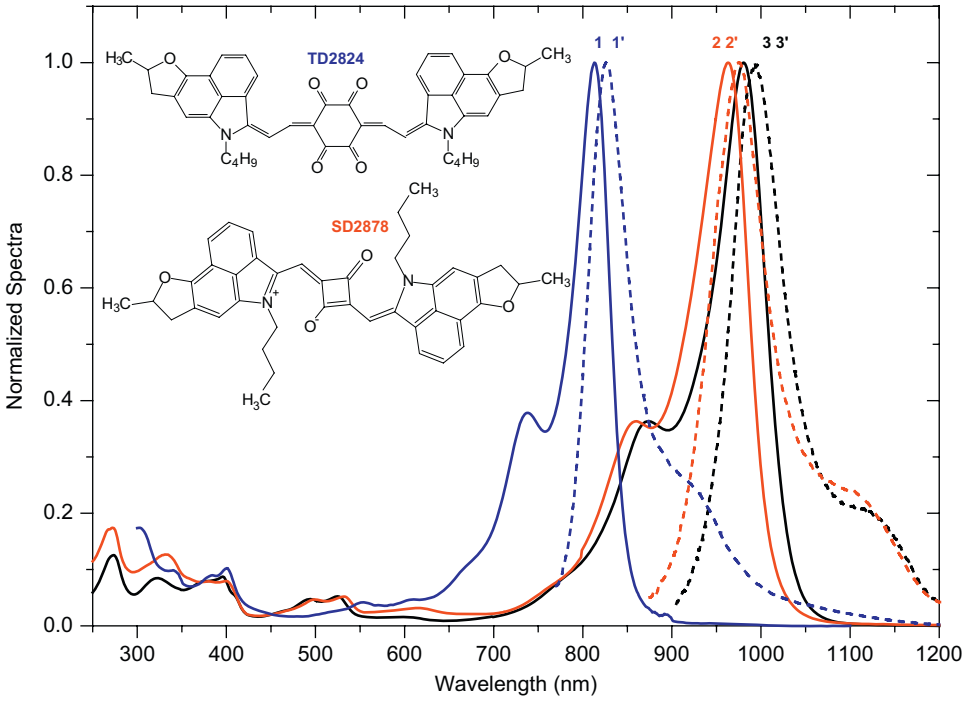

Fig. 3. Molecular structures, absorption (solid lines 1, 2, 3) and fluorescence spectra (dashed lines 1′, 2′, 3′) in butanol for TD 2824 (1, 1′), SD 2878 (2, 2′) and PD 2658 (3, 3′), respectively. *Note*: structure for PD 2658 is shown in Fig. 1(b).

Table 1
Spectroscopic characteristics of polymethine, squaraine and tetraone dyes in acetonitrile CH_3CN, dimethyl sulfoxide C_2H_6OS, butanol C_4H_9OH, dichloromethane CH_2Cl_2 and *o*-dichlorobenzene $C_6H_4Cl_2$; $\lambda_a^{max}(nm)$, position of absorption peak; $\lambda_f^{max}(nm)$, position of fluorescence peak; $\varepsilon^{max}(\times 10^5\,M^{-1}\,cm^{-1})$, extinction coefficient

Dye	CH_3CN			C_2H_6OS			C_4H_9OH			CH_2Cl_2			$C_6H_4Cl_2$		
	λ_a^{max} (nm)	$\varepsilon^{max}\times 10^5$ ($M^{-1}cm^{-1}$)	λ_f^{max} (nm)	λ_a^{max} (nm)	ε^{max} ($\times 10^5$ $M^{-1}cm^{-1}$)	λ_f^{max} (nm)	λ_a^{max} (nm)	ε^{max} ($\times 10^5$ $M^{-1}cm^{-1}$)	λ_f^{max} (nm)	λ_a^{max} (nm)	ε^{max} ($\times 10^5$ $M^{-1}cm^{-1}$)	λ_f^{max} (nm)	λ_a^{max} (nm)	ε^{max} ($\times 10^5$ $M^{-1}cm^{-1}$)	λ_f^{max} (nm)
PD 2371	870	1.08	898	–	–	–	885	0.99	893	–	–	–	908	1.31	918
PD 2658	969	1.62	998	–	–	–	980	2.11	991	–	–	–	1010	2.53	1029
PD 2716	1085	1.19	1119	–	–	–	1096	1.37	1109	–	–	–	1134	1.93	1158
PD 2892	1196	0.89	1247	1228	0.95	1260	1223	1.18	1263	1231	1.57	1269	1259	1.68	1279
SD 2878	–	–	–	–	–	–	963	1.71	975	–	–	–	–	–	–
TD 2824	–	–	–	–	–	–	813	1.76	828	–	–	–	–	–	–

region have been performed in two steps. First, we determined the fluorescence quantum yield for the photochemically stable polymethine dye 3-ethyl-2-[7-(3-ethyl-1,1-dimethyl-1,3-dihydro-2*H*-benzo[*e*]indol-2-ylidene)hepta-1,3,5-trienyl]-1,1-dimethyl-1*H*-benzo[*e*]indolium-4-methylbenzenesulfonate (we labeled it as PD 2631, see molecular structure in Fig. 4) in ethanol with an intermediate (between visible and near IR dyes) position of its absorption peak at 784 nm and the fluorescence maximum at 809 nm, using the Cresyl Violet dye as a standard. We chose this dye as an intermediate quantum yield "standard" for the longer absorbing molecules. Its absorption and fluorescence spectra in comparison with Cresyl Violet are shown in Fig. 4. Our measurements yield $\eta = 0.11 \pm 0.01$ for PD 2631. We next measure the fluorescence of the near IR dyes in comparison with that of the intermediate "standard" PD 2631. The optical densities of the absorption peaks in all cases were below 0.1 ensuring that reabsorption due to the small Stokes shifts does not play a dominant role in the measurement. We found that fluorescence quantum yields for all our dyes are very small in all solvents but are still measurable due to the high sensitivity of the cooled Hamamatsu photomultiplier. The quantum yields systematically decrease with increasing chain lengths. Their values are: $(2-3)\times 10^{-3}$ for PD 2371, $(4-8)\times 10^{-4}$ for PD 2658, $(1-2)\times 10^{-4}$ for PD 2716, $(1-2)\times 10^{-5}$ for PD 2892, $(6-7)\times 10^{-3}$ for TD 2824, and $(4-6)\times 10^{-4}$ for SD 2878 in butanol. From these measurements we can estimate fluorescence lifetimes, $\tau_F = \eta\tau_R$, where the natural lifetime, τ_R, can be calculated by the known formula [18]:

$$\frac{1}{\tau_R} = 2.88 \times 10^{-9} n^2 \varepsilon^{max} \left[\frac{\int F(\nu)\,d\nu \times \int(\varepsilon(\nu)/\nu)\,d\nu}{\int (F(\nu)/\nu^3)\,d\nu}\right], \quad (1)$$

where $F(\nu)$ and $\varepsilon(\nu)$ are normalized fluorescence and absorption spectra and ε^{max} is the extinction coefficient at the absorption peak. Estimated fluorescence lifetimes are: 25 ± 5 ps for PD 2371, 7.5 ± 2.5 ps for PD 2658, 3 ± 1 ps for 2716, <1 ps for PD 2892, 45 ± 5 ps for TD 2824 and 7.5 ± 2.5 ps for SD 2878. These values are compared with the lifetime values measured by a femtosecond pump-probe spectroscopic technique (data will be presented in our next paper, Ref. [26]) and the results agree within ~50%. These very small quantum yields and short lifetimes may be connected with the excited-state symmetry breaking. Our previous quantum-chemical calculations have shown that in the excited state, the dimension of the solitonic wave becomes smaller and therefore the symmetry breaking effect can occur for shorter polymethine chains [7]. Therefore, in accord with the theoretical studies performed for cyanine dyes in Ref. [22], we suggest that the most efficient route of energy deactivation is via formation of the asymmetrical molecular geometry, which is strongly coupled to the ground state geometry. However, these results need additional theoretical studies and experimental confirmation: for example, low temperature and time-resolved measurements.

Values for the transition dipole moments μ_{01} for all molecules are calculated from the integrated main absorption band $S_0 \rightarrow S_1$ [18], $\mu_{01} = \{[1500(\hbar c)^2 \ln 10]\int \varepsilon_{01}(\nu)\,d\nu]/\pi N_A E_{01}\}^{1/2}$, where $\varepsilon_{01}(\nu)$ is the extinction coefficient, N_A is Avogadro's number, and E_{01} is the peak energy. Calculations show that all dyes have similar μ_{01} values: 12 D for PD 2371, 16 D for PD 2658, 15 D for PD 2716, 18 D for PD 2892, 15 D for SD 2878 and 15 D for TD 2824 in butanol indicating a similar nature of the main ground to excited state transition $S_0 \rightarrow S_1$.

Fig. 5 represents a comparison between "near IR" (with dihydrobenzo[*cd*]furo[2,3-*f*]indolium terminal groups) and "visible" (with benzo[*e*]indolium terminal groups) sets of dyes. A distinguishing feature seen from Fig. 5 is a remarkably large red shift (~300 nm) of the absorption bands of PD 2658 and SD 2878 as compared to PD 2630 and SD 2243. The absorption spectrum of TD 2824 is red-shifted by ~200 nm as compared to TD 2765. These

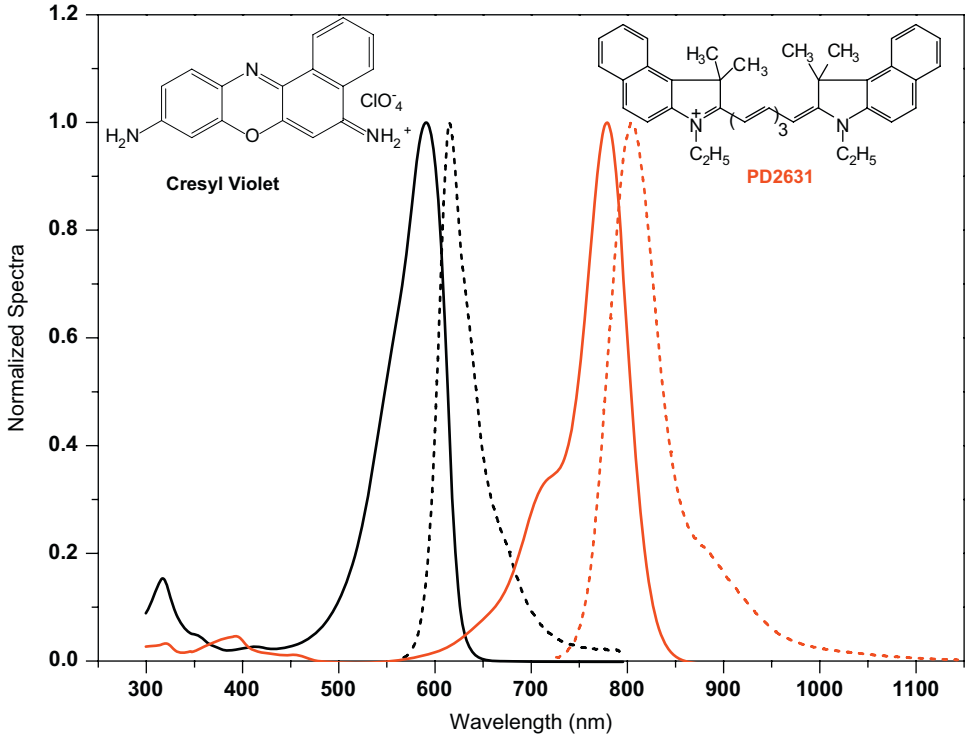

Fig. 4. Molecular structures, absorption (solid lines) and fluorescence spectra (dashed lines) of the quantum yield standard for the red region Cresyl Violet in methanol and the proposed "intermediate standard" PD 2631 in ethanol.

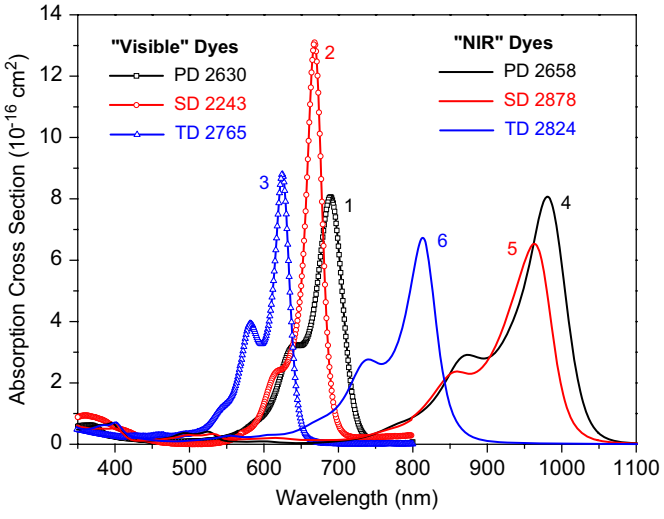

Fig. 5. Absorption spectra of the "Visible" set of dyes: PD 2630 (1), SD 2243 (2), TD 2765 (3) and "NIR" set of dyes: PD 2658 (4), SD 2878 (5), and TD 2824 (6). All in solutions of butanol.

large red shifts for the "near IR" set of molecules can be explained using two reasons: the extended π-system within the terminal groups, which is seen from the relatively long wavelength absorption of the salt 2337 (absorption peak is at 500 nm), and its strong conjugation with the π-system of the chain. This last statement is discussed in Section 3.

3. Quantum-chemical analysis

Quantum-chemical orbital analysis is performed with the goal of understanding the formation of the linear absorption spectra in the series of near IR dyes with dihydrobenzo[*cd*]furo[2,3-*f*]indolium terminal groups and their comparison with the "visible" set of dyes. The methodology for the calculations of the positions of the electronic levels and the shapes of their molecular orbitals is described in Refs. [15,16]. This orbital approach is a very useful tool for understanding the nature of the orbitals and their origins, as well as the nature of the transitions between them. It was applied by us earlier for the series of visible dyes (PD 2630, SD 2243, and TD 2765) [17] and allowed for a considerably clearer picture of structure–property relations. Fig. 6 shows the optimized molecular geometries for the "visible" and "near IR" set of molecules calculated in the HyperChem, AM1 approximation [23]. The corresponding bond lengths are presented in Tables 2 and 3. There are several important conclusions from the analysis of the bond lengths and bond length difference or alternation (BLA). First, a minimum BLA is observed for all PDs within the chain, which is a typical feature of polymethine molecules as described in S. Dähne's "Triad theory" [24]. Second, incorporation of the squaraine acceptor bridge to the polymethine chromophore in SD 2243 and SD 2878 causes the appearance of BLA within the bridge and results in a blue shift (≈20 nm) of the absorption bands as compared to the corresponding PDs. Incorporation of the stronger tetraone acceptor units to TD 2765 and TD 2824 leads to a larger BLA within the bridge and changes the nature of the molecules from the odd polymethine system to the even polyenic type of conjugation. Therefore, BLA is seen within the whole conjugated system (not only in the bridge), and the absorption spectra of TDs are more blue-shifted, especially for the "near IR" TD 2824 (~170 nm), as compared to the corresponding PD 2658 (see Fig. 3). The next important conclusion from the analysis of BLA relates to the conjugation between the terminal groups and the main chromophore. As can be seen from Table 3, the bond lengths between C11 and C16 (1.552 Å), and between C10 and C11 (1.519 Å) in the benzo[*e*]indolium terminal groups disconnect the conjugation with the main chromophore, and conjugation

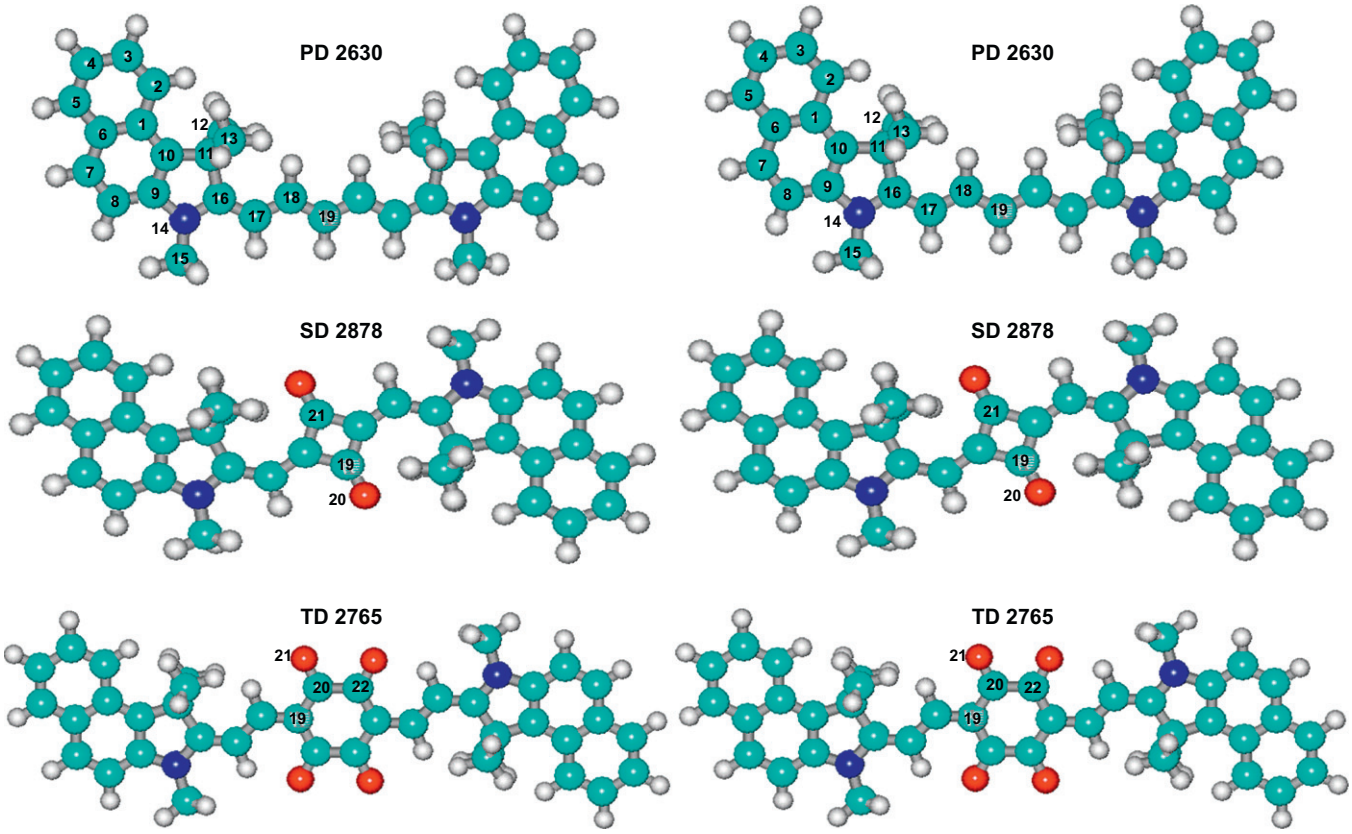

Fig. 6. The optimized molecular geometries for the "visible" and "near IR" set of the molecules (HyperChem, AM1 approximation). Light blue are carbon atoms, dark blue are nitrogen atoms, red are oxygen atoms, and white are hydrogen atoms. The atom numbers are shown in figure and the bond lengths are shown in Tables 2 and 3.

Table 2
Calculated bond lengths (in Å) for the "near IR" set of dyes PD 2658, SD 2878, and TD 2824

Segment	Bond number	PD 2658	SD 2878	TD 2824
Terminal groups	C1–C2	1.509	1.509	1.509
	C2–O3	1.465	1.460	1.469
	O3–C4	1.375	1.386	1.384
	C4–C5	1.411	1.406	1.404
	C5–C6	1.496	1.495	1.492
	C2–C6	1.540	1.539	1.546
	C5–C7	1.403	1.405	1.406
	C4–C8	1.416	1.416	1.416
	C8–C9	1.420	1.423	1.423
	C9–C10	1.382	1.379	1.378
	C10–C11	1.422	1.425	1.426
	C11–C12	1.377	1.373	1.373
	C12–C13	1.439	1.439	1.438
	C8–C13	1.401	1.400	1.400
	C13–C14	1.433	1.438	1.439
	C7–C14	1.403	1.387	1.384
	C14–N15	1.423	1.411	1.411
	N15–C16	1.430	1.425	1.425
	N15–C17	1.396	1.422	1.416
	C12–C17	1.484	1.481	1.490
Chain	C17–C18	1.398	1.379	1.369
	C18–C19	1.391	1.383	1.413
	C19–C20	1.398		1.372
Acceptor bridge	C19–C20		1.468	
	C19–C22		1.488	
	C20–C21			1.462
	C21–C23			1.512
	C20–O21		1.233	
	C21–O22			1.241

AM1 approximation. The atom numbers are shown in Fig. 6.

Table 3
Calculated bond lengths (in Å) for the "visible" set of dyes PD 2630, SD 2243, and TD 2765

Segment	Bond number	PD 2630	SD 2243	TD 2765
Terminal group	C1–C2	1.423	1.424	1.425
	C2–C3	1.372	1.370	1.371
	C3–C4	1.416	1.417	1.417
	C4–C5	1.372	1.372	1.371
	C5–C6	1.424	1.424	1.423
	C6–C7	1.421	1.420	1.419
	C7–C8	1.377	1.377	1.375
	C8–C9	1.413	1.415	1.414
	C9–C10	1.407	1.400	1.411
	C10–C11	1.519	1.517	1.520
	C11–C12	1.517	1.517	1.518
	C11–C13	1.517	1.517	1.518
	C9–N14	1.425	1.414	1.409
	N14–C15	1.433	1.427	1.428
	N14–C16	1.375	1.400	1.400
	C11–C16	1.552	1.545	1.547
Chain	C16–C17	1.395	1.376	1.366
	C17–C18	1.392	1.389	1.415
	C18–C19	1.392		1.371
Acceptor bridge	C18–C19		1.482	
	C18–C21		1.473	
	C19–C20			1.464
	C20–C22			1.510
	C19–O20		1.233	
	C20–O21			1.239

AM1 approximation. The atom numbers are shown in Fig. 6.

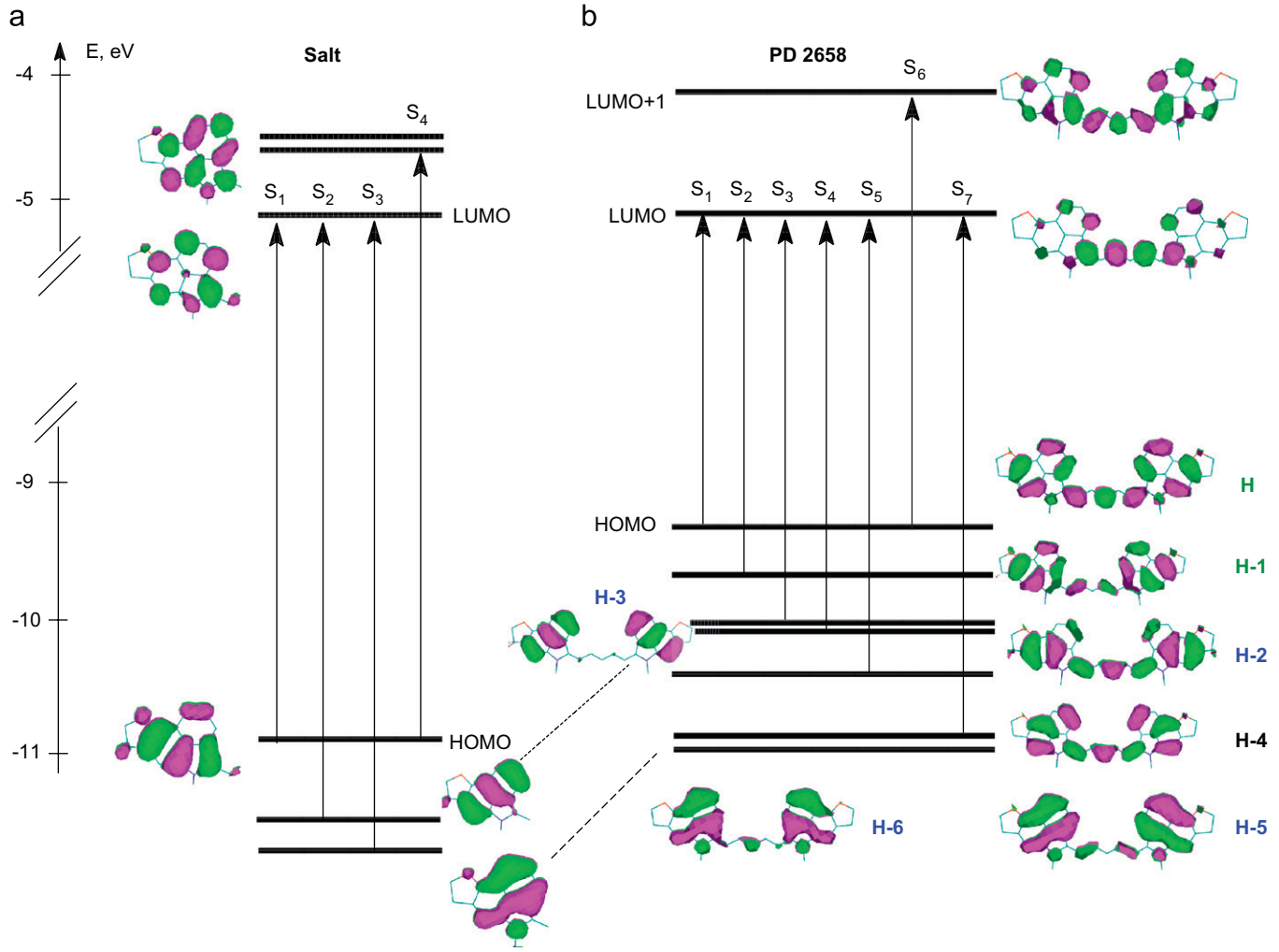

Fig. 7. Scheme of molecular orbital energy levels, transitions and electron density distribution for the salt 2337 (a) and PD 2658 (b).

takes place mainly through the donor nitrogen atoms. In contrast, dihydrobenzo[*cd*]furo[2,3-*f*]indolium terminal groups have a much stronger connection to the chain (the longest corresponding bond C12–C17 does not exceed 1.484 Å), resulting in the extension of the effective conjugation length (see Table 2). The effect of these terminal groups is equivalent to the extension of the chain to three vinylene groups specifically for PDs with benzo[*e*]indolium terminal groups.

The energies of the molecular orbitals (MOs), electronic transitions between them and oscillator strengths were calculated in the framework of the standard semi empirical ZINDO/S method [25]. The wavefunctions of the excited states were built with the configuration interaction technique taking into account seven occupied and three unoccupied MOs, a total of 21 configurations, which has been shown to be enough for the spectral characterization of the dyes studied in the near UV, visible and near IR ranges.

Fig. 7 represents the schemes of the highest occupied MO (HOMO), several occupied MOs below HOMO, lowest unoccupied molecular orbital (LUMO), several unoccupied MO over LUMO, the shapes of MOs, and corresponding transitions between them for PD 2658 in comparison with the orbitals of the salt 2337. The wave function of the *i*th MO φ_i was written as an expansion of the atomic orbitals $\chi_\mu : \varphi_i = \sum_\mu C_{i\mu}\chi_\mu$, where the $C_{i\mu}$ are the corresponding coefficients, and the summation runs over all atomic orbitals. We note that $C^2_{i\mu}$ is the probability of the location of an electron in the *i*th MO in the neighborhood of the μth atom [16]. The shapes of MOs presented in Fig. 7 correspond to coefficients $C_{i\mu}$, allowing to analyze the symmetry of the wave function φ_i.

Quantum-chemical orbital analysis allows a distinction between three types of molecular orbitals: (1) two donor occupied orbitals, HOMO and HOMO-1, originating from the donor nitrogen atoms and extending to the chain due to the effect of the terminal groups; (2) local occupied and unoccupied orbitals, originating primarily from the benzene rings of the terminal groups (HOMO-2, HOMO-3); and (3) delocalized occupied and unoccupied orbitals spreading out over the chain (LUMO) or the entire molecule (HOMO-4). Note that symmetrical and asymmetrical pairs of donor and local orbitals are formed from the doubly degenerate orbitals as a result of their splitting, leading to charge redistribution. Therefore, transitions between corresponding orbitals are characterized by very different oscillator strengths. A more detailed description of the nature of different types of orbitals can be found in our previous article [16]. The first allowed $S_0 \rightarrow S_1$ transition for all molecules is connected with electron transfer from HOMO to LUMO. For PD 2658 (C_{2V} molecular symmetry) presented in Fig. 7, this is the $1A_1 \rightarrow 1B_1$ transition. It is important to take into account that the positions of the LUMO for all cationic molecules are almost independent of molecular topology. Charge is distributed over the chain only (compare LUMO positions of the salt and PD 2658). Therefore, this level may be presented as a level of charge, or solitonic level. As a result, we may conclude that the $S_0 \rightarrow S_1$ transition energy for all PDs

depends mainly on the position of the donor HOMO level. Note that this level may be shifted substantially for the neutral molecules, such as SDs and TDs. An increase in the chain length (corresponding to an increase of π-electrons) leads to a higher energy position of the HOMO and a decrease in the energy gap between the HOMO and LUMO. As a result, PDs with dihydrobenzo[*cd*]furo[2,3-*f*]indolium terminal groups are characterized by much longer wavelength positions of the absorption bands (≈300 nm longer) as compared to the dyes with the same length of the chain, but the simpler terminal groups, such as indolium or benzo[*e*]indolium, studied by us earlier [15–17]. This large red shift is connected with more extended conjugated systems in terminal groups moving their HOMO to higher energy positions.

The next $S_0 \rightarrow S_2$ transition for all dyes involve mostly the asymmetrical donor HOMO-1 and asymmetrical LUMO. This transition, being of $1A_1 \rightarrow 2A_1$ symmetry for PDs, is characterized by a much smaller oscillator strength and corresponds to experimentally observed less intense absorption bands at ≈570 nm for PD 2371, ≈615 nm in PD 2658, and ≈648 nm in PD 2716 in the less polar solvent *o*-dichlorobenzene (which more accurately corresponds to data from quantum-chemical calculations). In the tetracarbocyanine, PD 2892, this band is hidden by the shoulder of the $S_0 \rightarrow S_1$ band. We note that quantum-chemical calculations indicate a degeneracy and large splitting energy between the two donor molecular orbitals, HOMO and HOMO-1. This results in a large separation (>300 nm) between $S_0 \rightarrow S_1$ and $S_0 \rightarrow S_2$ transitions. In contrast, the corresponding distance for the visible dyes is <150 nm. Two next transitions, $S_0 \rightarrow S_3$ and $S_0 \rightarrow S_4$ for all dyes correspond to the electron transfer from the symmetrical HOMO-2 and asymmetrical HOMO-3 local orbitals to the LUMO. These bands originate from the molecular orbitals localized at the terminal groups and correspond to the lowest absorption band of the salt 2337 (peak position ≈492 nm, see Fig. 2). These local bands show a systematical red shift of ≈30 nm with an increase of the chain length from PD 2371 to PD 2892, without a substantial change in shape. This theoretical finding is in agreement with our observation of the so-called "blue" fluorescence, seen in the series of dyes and shown in Fig. 2. It is our understanding that this fluorescence originates from the $S_0 \rightarrow S_3$ local transition and is connected with the charge localization within the terminal groups. The next, $S_0 \rightarrow S_5$ transition involves charge transfer from HOMO-4, which is delocalized over the whole molecule, to the same LUMO level. The nature of the two next transitions, $S_0 \rightarrow S_6$ and $S_0 \rightarrow S_7$ for all molecules, is more complicated and mixed, involving transitions from HOMO-5 to LUMO and from HOMO to the higher LUMO+1 level. We note that the terminal groups are much more involved in all transitions as compared to dyes with indolium and benzo[*e*]indolium terminal groups, as can be seen not only from quantum-chemical calculations, but from a comparison of the visible and UV absorption spectra of near IR dyes and the corresponding salt (see Fig. 2).

4. Conclusions

We have described a detailed experimental investigation of the linear absorption and fluorescence spectra of a new series of near IR cationic polymethine dyes and performed quantum-chemical analyses in order to understand the effect of dihydrobenzo[*cd*]-furo[2,3-*f*]indolium terminal groups. We also synthesized and studied two neutral dyes, squaraine and tetraone, with the same terminal groups to provide a deeper insight into structure–property relations and get a better understanding of the properties of cyanine and cyanine-like molecules. We performed a comparison of the spectroscopic properties of the new series of "near IR" dyes (PD 2658, SD 2878, and TD 2824) with our previously studied series of "visible" dyes (PD 2630, SD 2243, and TD 2765) with the simpler benzo[*e*]indolium terminal groups. We find, from these measurements, that the dyes with dihydrobenzo[*cd*]furo[2,3-*f*]indolium terminal groups are characterized by a remarkably large red shift of their main absorption bands of about ≈300 nm (≈200 nm for tetraone). Experimental and quantum-chemical analyses allow us to make the following conclusions:

1. The large red shifts for the absorption bands in the "near IR" set of molecules can be explained by the extended π-system in the terminal groups, which strongly conjugates with the π-system of the chain resulting in a substantial extension of the effective conjugation length. The effect of these terminal groups is equivalent to the extension of the chain to three vinylene groups specifically for PDs with benzo[*e*]indolium terminal groups.
2. Introduction of the acceptor squaraine and tetraone bridges to the conjugated chain causes a bond-length alternation (BLA) in the bridges resulting in a blue shift of the main absorption bands. Additionally, an incorporation of the stronger tetraone acceptor units to TD 2765 and TD 2824 leads to a larger BLA within the bridge and changes the nature of the molecules from the polymethine to the polyenic type of conjugation. Therefore, BLA for tetraones is observed within the whole conjugated system, and their absorption spectra are more blue-shifted, especially for the near IR TD 2824, as compared to the corresponding PD 2658.
3. Absorption spectra for the longest PD 2716 and PD 2892 dyes are solvent-dependent and are characterized by a significant broadening of the main band, $S_0 \rightarrow S_1$, in polar solvents. Quantum-chemical calculations explain this effect by ground state symmetry breaking and reduced charge delocalization within the polymethine chromophore. Experiments show that the less polar solvent primarily stabilizes the symmetric form. An increase of solvent polarity leads to an increase in the relative concentration of the asymmetric form. In contrast to the absorption spectra, fluorescence spectra for all PDs are similarly narrow, independent of the solvent polarity, indicating that the emission originates from the symmetrical form only.
4. All near IR dyes are characterized by a very small fluorescence quantum yield, $\sim 10^{-3}$ to 10^{-5}, and very short fluorescence lifetimes from ~1 ps for PD 2892 to ~50 ps for TD 2824 which may be connected with energy deactivation via an excited state asymmetrical geometry. However, this conclusion needs more detailed low temperature and time-resolved fluorescence studies.
5. Near IR polymethines show an emission from the higher lying excited states, which is situated in the range from ~500 to 650 nm and show similarity to that of the salt 2337. Our explanation, based on the experimental and theoretical results, suggests that this "blue" fluorescence originates from the local orbitals connected with the terminal groups.

These studies have advanced our understanding of the structure–property relations in conjugated cyanine-like molecules, which are extremely important for understanding the nonlinear optical behavior of these dyes and their associated nonlinear optical applications to be discussed in our next paper [26].

Acknowledgments

We gratefully acknowledge the support of the National Science Foundation ECS 0524533, the US Army Research Laboratory W911NF0420012, the US Army Research Laboratory and the US

Army Research Office under contract/grant number 50372-CH-MUR, and the Office of Naval Research MORPH N00014-06-1-0897.

References

[1] A. Mishra, Chem. Rev. 100 (2000) 1973.
[2] F. Meyers, S.R. Marder, J.W. Perry, Chemistry of Advanced Materials, Wiley-VCH, New York, 1998.
[3] J.M. Hales, S. Zheng, S. Barlow, S.R. Marder, J.W. Perry, J. Am. Chem. Soc 128 (2006) 11362.
[4] J. Fabian, Chem. Rev. 92 (1992) 1197.
[5] A.I. Tolmachev, Yu.L. Slominsky, A.A. Ishchenko, in: S. Daehne, U. Resch-Genger, O.S. Wolfbeis (Eds.), Near-Infrared Dyes for High Technology Applications, vol. 52, Kluwer Academic Publishers, New York, 1998.
[6] L.M. Tolbert, X. Zhao, J. Am. Chem. Soc. 119 (1997) 3253.
[7] R.S. Lepkowicz, O.V. Przhonska, J.M. Hales, J. Fu, D.J. Hagan, E.W. Van Stryland, M.V. Bondar, Yu.L. Slominsky, A.D. Kachkovski, Chem. Phys. 305 (2004) 259.
[8] A. Yu, C. Tolbert, D. Farrow, D. Joneas, J. Phys. Chem. A 106 (2002) 9407.
[9] A.B. Ryabitsky, A.D. Kachkovski, O.V. Przhonska, THEOCHEM 802 (2007) 75.
[10] J. Fabian, THEOCHEM 766 (2007) 49.
[11] J.S. Craw, J.R. Reimers, G.B. Bacskay, A.T. Wong, N.S. Hush, Chem. Phys. 167 (1992) 77.
[12] J.S. Craw, J.R. Reimers, G.B. Bacskay, A.T. Wong, N.S. Hush, Chem. Phys. 167 (1992) 101.
[13] I.G. Davydenko, Yu.L. Slominsky, A.D. Kachkovski, A.I. Tolmachev, Polymethine dyes derived from 7,8-dihydrobenzo[*cd*]furo[2,3-*f*]indole, Ukr. Khim. Zh. 74 (2008) 105.
[14] I.G. Davydenko, Yu.L. Slominsky, A.D. Kachkovski, A.I. Tolmachev, The nature of electron transitions in cyanine dyes, derivatives of 7,8-dihydrobenzo[*cd*]-furo[2,3-*f*]indole, Ukr. Khim. Zh. 74 (2008) 110.
[15] J. Fu, L.A. Padilha, D.J. Hagan, E.W. Van Stryland, O.V. Przhonska, M.V. Bondar, Yu.L. Slominsky, A.D. Kachkovski, JOSA B 24 (2007) 56.
[16] J. Fu, L.A. Padilha, D.J. Hagan, E.W. Van Stryland, O.V. Przhonska, M.V. Bondar, Yu.L. Slominsky, A.D. Kachkovski, JOSA B 24 (2007) 67.
[17] S. Webster, J. Fu, L.A. Padilha, O.V. Przhonska, D.J. Hagan, E.W. Van Stryland, M.V. Bondar, Yu.L. Slominsky,, A.D. Kachkovski, Chem. Phys. 348 (2008) 143.
[18] J.R. Lakowicz, Principles of Fluorescence Spectroscopy, second ed., Kluwer Academic/Plenum Publishers, New York, 1999.
[19] R.S. Lepkowicz, O.V. Przhonska, J.M. Hales, D.J. Hagan, E.W. Van Stryland, M.V. Bondar, Yu.L. Slominsky, A.D. Kachkovski, Chem. Phys. 286 (2003) 277.
[20] R.S. Lepkowicz, O.V. Przhonska, J.M. Hales, D.J. Hagan, E.W. Van Stryland, M.V. Bondar, Yu.L. Slominsky, A.D. Kachkovski, JOSA B 22 (2005) 2664.
[21] D. Magde, J.H. Brannon, T.L. Cremers, J. Olmsted, J. Phys. Chem. 83 (1979) 696.
[22] A. Sanchez-Galvez, P. Hunt, M.A. Robb, M. Olivucci, T. Vreven, H.B. Schlegel, J. Am. Chem. Soc. 122 (2000) 2911.
[23] M.J.S. Dewar, E.G. Zoebisch, E.F. Healy, J.J.P. Stewart, J. Am. Chem. Soc. 107 (1985) 3902.
[24] S. Dähne, Science 199 (1978) 1163.
[25] M.C. Zerner, G.H. Loew, R.F. Kirchner, U.T. Mueller-Westerhoff, J. Am. Chem. Soc. 102 (1980) 589.
[26] L.A. Padilha, S. Webster, H. Hu, O.V. Przhonska, D.J. Hagan, E.W. Van Stryland, M.V. Bondar, I.G. Davydenko, Yu.L. Slominsky, A.D. Kachkovski, Chem. Phys. (2008), in press, doi:10.1016/j.chemphys.2008.05.007.